

Computational and Experimental Analysis for Horizontal Axis Marine Current Turbine Design

Ju Hyun Lee¹, Dong Hwan Kim¹, Shin Hyung Rhee^{1,2},
In Rok Do³, Byung Chul Shin³, and Moon Chan Kim³

¹Dept. of Naval Architecture & Ocean Engineering, Seoul National University, Seoul, Korea

² Research Institute of Marine Systems Engineering, Seoul National University, Seoul, Korea

³ Dept. of Naval Architecture & Ocean Engineering, Pusan National University, Busan, Korea

ABSTRACT

Performance analysis methods for the design of horizontal axis marine current turbines were developed using computational and experimental methods. For the computational analysis, two methods were utilized: (1) the blade element momentum theory (BEMT) method, and (2) the computational fluid dynamics (CFD) method, based on the Reynolds-averaged Navier-Stokes equations. For the experimental analysis, open water tests were carried out in a towing tank. First, the computational methods were validated by comparing with the existing experimental data. Then the computational analysis results for the selected model turbine were compared to the experimental results, demonstrating good ability of performance prediction. Finally, using the validated computational method, new designs for the blade tip were suggested and their hydrodynamic performance was predicted. The new raked tip design suggests delay of the tip cavitation inception near the free surface.

Keywords

Horizontal axis marine current turbine design, Blade element momentum theory (BEMT), Computational fluid dynamics (CFD), Raked tip blade

1 INTRODUCTION

Recently, due to high oil prices and environmental pollution issues, interest in the development of the alternative energy has increased tremendously. The marine current turbine, which utilizes marine current energy, has many attractive features and is known as one of the most promising energy conversion devices. It is reliable, predictable and has the potential for minimizing both visual and noise pollution (McCleod et al 2002). The energy conversion turbine systems can be categorized primarily into horizontal and vertical axis, with respect to

its rotor axis configuration. The horizontal axis turbine, where the rotating axis is parallel to incoming flow, has many merits compared to the vertical axis turbine. The wind turbine and marine propeller industries have carried out an abundance of earlier studies on horizontal axis machinery. Also, the pitch control system to protect the rotor in overly high inflow speed is easier to adopt. Though the vertical axis turbine also has advantages in manufacturing and maintenance, its drawbacks in the structural robustness have always been a burden in competing with the horizontal axis turbine. The horizontal axis turbine, therefore, was believed to be a better choice, and thus, studied in this paper.

For the design of a horizontal axis marine current turbine, performance analysis is essential. Though a lot of studies are found on wind turbines and marine propellers, only a few studies were conducted for the performance analysis of marine current turbines. The performance analysis methods are mainly divided into computational and experimental ones. For the computational methods, BEMT and CFD are mostly used. Coiro et al (2006) and Batten & Bahaj (2008) developed performance prediction codes based on BEMT and also performed experimental analyses in a towing tank. Mason-Jones et al (2008) and Kinnas & Xu (2009) presented three-dimensional (3D) turbine performance analysis results using CFD. Harrison (2009) analyzed the wake effects of a turbine by CFD. Liu (2010) used the panel method and McCombes et al (2009) used the vorticity-pressure-based CFD method for turbine performance analysis.

For the design of a horizontal axis marine current turbine from the concept to final design stage, performance analysis methods using both computational and experimental methods were developed in the present study. The computational methods were used to predict the turbine performance for various design parameters,

while the experimental method was employed to confirm the selected turbine's performance.

Computational analysis was done with BEMT and CFD methods. BEMT method, which models a rotor as a set of isolated two-dimensional (2D) blade elements, is a very cost-effective method for a rough prediction of turbine performance, but it cannot provide detailed information on the flow field of the surrounding region. CFD method, on the other hand, is able to predict accurately not only the hydrodynamic performance of the turbine, but also the velocity and pressure distribution around the turbine blades. BEMT code was validated by comparing with the performance analysis results of another BEMT program, WT_Perf (Buhl 2009), for four different turbines. CFD method was validated by comparing with the existing experiment data.

The computational methods were applied to the selected model turbine and the results were compared with experimental analysis results. Experimental analysis for the performance prediction was done in a towing tank by conducting open water tests for the horizontal axis marine current turbine. Then the computational methods were applied for new blade tip designs, proposed to delay the tip vortex cavitation inception without degrading the turbine performance.

The paper is organized as follows. First, the description and validation of the two computational methods are given. The experimental setup and methods are described next. Then both the computational and experimental results for the selected model turbine are presented and compared. The proposed new blade tip designs and their performance are discussed. Finally, concluding remarks are made.

2 COMPUTATIONAL METHODS

2.1 Blade element momentum theory

BEMT is one of the most practical tools to predict aero/hydrodynamic performance of horizontal axis turbines and has been used in turbine design and analysis for many years. It basically combines the momentum theory and the blade element theory, and determines the axial and tangential induction factors for the independent blade sections in the span-wise direction using 2D aero/hydrodynamic characteristics. The developed BEMT code determines the induction factors using the following Equation (1):

$$\frac{aF}{1-a} = \frac{\sigma_r}{4\sin^2 \phi} \left[C_x - \frac{\sigma_r C_y^2}{4\sin^2 \phi} \right] \quad (1)$$

$$\frac{a'F}{1+a'} = \frac{\sigma_r C_y}{4\sin \phi \cos \phi}$$

where a = axial induction factor;

a' = tangential induction factor;

F = tip-hub loss factor;

σ_r = local solidity;

C_x = normal force coefficient;

C_y = tangential force coefficient;

$$\phi = \text{incident flow angle.}$$

In order to consider the tip and hub loss effects, Prandtl's tip loss factor was taken as:

$$F_{tip} = \frac{2}{\pi} \cos^{-1} \left(\exp \left(-\frac{B}{2\sin \phi} \frac{1-x}{x} \right) \right) \quad (2)$$

$$F_{hub} = \frac{2}{\pi} \cos^{-1} \left(\exp \left(-\frac{B}{2\sin \phi} \frac{x-x_{hub}}{x} \right) \right)$$

where B = number of blades;

x = non-dimensionalized radial length.

For the calculation of the induction factors in the turbulent windmill state, the thrust coefficient curve of GH-BLADED was taken as follows.

$$C_T = 0.79a^2 + 0.61a + 0.6 \quad (a > 0.3539) \quad (3)$$

The hydrodynamic characteristics for the computation were obtained using 2D CFD results. The representative Reynolds number, based on the relative inflow velocity and rotor diameter, was determined to be six million at the design TSR. For the post stall region, the Viterna-Corriigan method (Viterna & Corriigan, 1978) was used right after the stall.

2.2 Computational fluid dynamics

BEMT is a cost-effective method for roughly calculating the turbine performance, but it cannot provide a detailed and more precise solution because of its simplicity. To obtain more reliable prediction results, 3D CFD analysis was performed. In the present study, a rotating reference frame was employed to deal with the rotating characteristic of the rotor. The rotating reference frame is one of the simplest approaches for modeling problems that involve rotating zones.

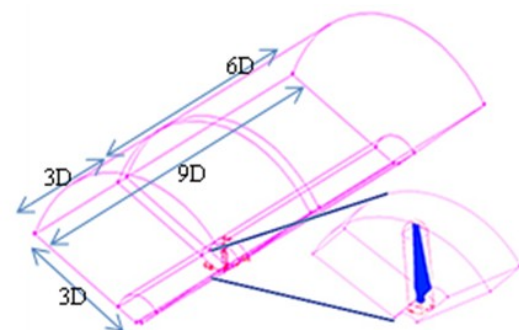


Figure 1: Computational domain

Figure 1 shows the computational domain for the turbine performance analysis. Computation was done with only one blade and 120-degree section, because the inflow was uniform and the rotor blades were periodically located. The computational domain extent was 9D in length and 3D in radius, where D represents the turbine diameter. A hybrid mesh was used, where the domain was divided into several sub-domains: one with complex blade geometry, enlarged in Figure 1, was filled with tetrahedral cells and the others having simple geometry was filled with

hexahedral cells for high quality solution. The analysis was done for various TSR's by keeping the inflow speed constant and varying the rotational speed.

3 VALIDATION OF COMPUTATIONAL METHODS

3.1 Validation of BEMT code

To validate the developed BEMT code, the obtained power coefficients were compared to those calculated by WT_Perf (Buhl 2009). Figure 2 shows the comparison of the power coefficients, displaying good agreement at different set angles in a wide range of TSR.

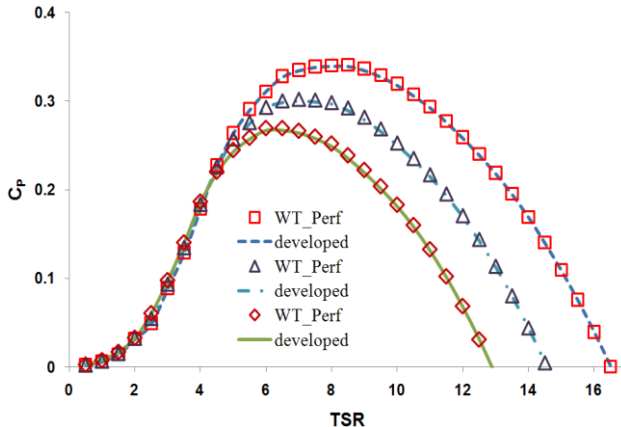


Figure 2: Comparison between BEMT code and WT_Perf.

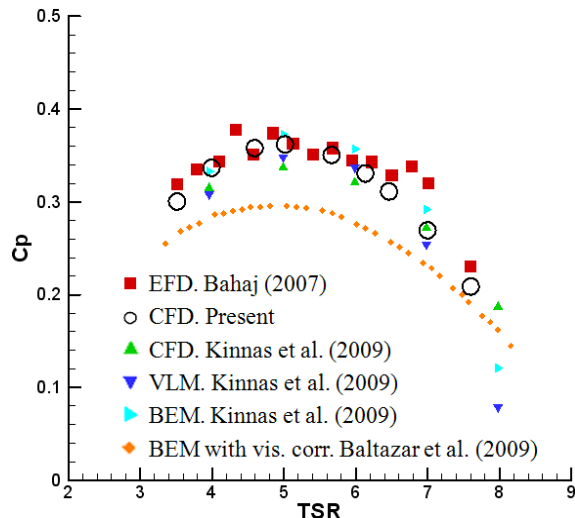


Figure 3: Validation results

3.2 Validation of CFD method

For the validation of CFD method, the computational results were compared with the existing experiment data obtained by Bahaj et al (2007), who carried out model tests in a 2.4 m × 1.2 m test section cavitation tunnel and 60 m long towing tank. The model turbine's diameter was 800 mm diameter, and consisted of three blades developed from five different NACA64-8XX series airfoil sections. The geometry modeling of the turbine for computational analysis was done with CATIA. Computational analysis was carried out with the same condition for the experiment. Figure 3 shows the performance analysis results. The results of the vortex lattice method (VLM) by Kinnas & Xu (2009) and the

boundary element method (BEM) by Kinnas & Xu (2009) and Baltazar & Falcao de Campos (2009) are also included. The present CFD results agree well with the experimental data and seemed more accurate than other numerical methods.

4 EXPERIMENTAL SETUP AND METHOD

Model tests were carried out in the towing tank at Pusan National University, which is 100 m long, 8 m wide and 3.5 m deep. The maximum towing speed of the carriage is 5m/s and the maximum acceleration is 2m/s². The test rig device in Figure 4 was manufactured and attached to the carriage.



Figure 4: Test rig

To predict the turbine performance, measurements of torque and revolution speed in rpm were needed. To measure the torque and revolution of the model turbine, the torque sensor, rpm sensor and powder break devices were adopted. The torque sensor and rpm sensor in Figure 5 (a), which can measure up to 10 kgf-m and 10,000 rpm, respectively, were equipped in the torque transducer located at the bottom of the test rig's upper cover. The powder break device, controlled by powder break controller in Figure 5 (b), could resist the shaft rotation and control the revolution speed. Using the powder break in Figure 5 (c), the torque of the turbine was measured in two ways: (1) fixed rpm method, i.e., measuring torque at varying carriage speed with constant shaft revolution speed, and (2) fixed speed method, i.e., measuring torque at constant carriage speed with break-free revolution speed.

Before the measurement, calibration was done and it was confirmed that the one-to-one proportional digital signal to voltage signal was produced. Measurements for the hydrodynamic performance were done using fixed rpm method, i.e., carriage speed varied and powder break kept rpm constantly. To examine the Reynolds number effects, measurements were also done with increasing rpm. The selected rpm was determined by considering the towing speed and was 250, 310, 420 rpm in the present experiment.

Table 1: Geometry of the reference blade

r/R	Chord length (mm)	Twist angle (degree)	Section info.
0.15	300.00	0.00	2:1 Elliptic cylinder
0.20	300.00	0.00	2:1 Elliptic cylinder
0.25	transient	transient	transient
0.30	684.11	16.98	NACA 63-418
0.35	655.11	14.59	NACA 63-418
0.40	626.11	12.66	NACA 63-418
0.45	597.10	11.07	NACA 63-418
0.50	568.10	9.75	NACA 63-418
0.55	539.10	8.64	NACA 63-418
0.60	510.09	7.69	NACA 63-418
0.65	481.09	6.87	NACA 63-418
0.70	452.09	6.15	NACA 63-418
0.75	423.08	5.50	NACA 63-418
0.80	394.08	4.91	NACA 63-418
0.85	365.08	4.33	NACA 63-418
0.90	336.08	3.74	NACA 63-418
0.95	307.07	3.02	NACA 63-418



Figure 5 Measurement devices

5 PERFORMANCE ANALYSIS OF THE MODEL TURBINE

5.1 Model Turbine

A model scale horizontal axis turbine with three blades shown in Figure 4 was considered. The blade geometry of the full scale rotor is given in Table 1. The scale factor was determined to be 11.428 considering the size of the towing tank. The radius of the model turbine was 0.7 m. The cone shaped rotor nose was taken from many other tidal current turbines and wind turbines. The non-dimensional parameters such as TSR, power coefficient, torque coefficient, Reynolds number are defined as:

$$\begin{aligned} \lambda &= \frac{R\Omega}{V_M} = \frac{\pi Dn}{60 \cdot V_M} & C_Q &= \frac{Q}{\frac{1}{2} \rho \pi R^2 V_M^2} \\ C_P &= \frac{Q\Omega}{\frac{1}{2} \rho \pi R^2 V_M^3} & R_n &= \frac{l_{0.7R} V_R}{v} \end{aligned} \quad (4)$$

where R = radius;

Ω = rotational speed;

V_M = model speed;

Q = torque;

$l_{0.7R}$ = chord length at $0.7R$;

V_R = relative inflow speed ($\sqrt{VM^2 + (0.7\pi nD)^2}$);

v = kinematic coefficient of viscosity.

The representative turbine radius for the Reynolds number was determined to be $0.7R$, following the example in marine propellers.

Table 1: Geometry of the reference blade

r/R	Chord length (mm)	Twist angle (degree)	Section info.
0.15	300.00	0.00	2:1 Elliptic cylinder
0.20	300.00	0.00	2:1 Elliptic cylinder
0.25	transient	transient	transient
0.30	684.11	16.98	NACA 63-418
0.35	655.11	14.59	NACA 63-418
0.40	626.11	12.66	NACA 63-418
0.45	597.10	11.07	NACA 63-418
0.50	568.10	9.75	NACA 63-418
0.55	539.10	8.64	NACA 63-418
0.60	510.09	7.69	NACA 63-418
0.65	481.09	6.87	NACA 63-418
0.70	452.09	6.15	NACA 63-418
0.75	423.08	5.50	NACA 63-418
0.80	394.08	4.91	NACA 63-418
0.85	365.08	4.33	NACA 63-418
0.90	336.08	3.74	NACA 63-418
0.95	307.07	3.02	NACA 63-418

5.2 Analysis Results

The measured data and computational results are presented in Figure 6. The results of BEMT and CFD were very close to each other around the design TSR. The peak power was predicted around the TSR of 0.46 for both cases. The differences between the experimental and computational results are considered mainly as Reynolds number effects. It should also be noted that due to the friction loss in the gear, the torque was slightly under-measured.

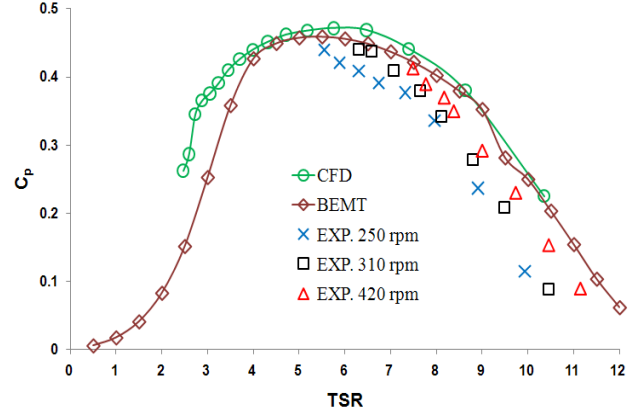


Figure 6: Comparison of numerical and experiment data

6 RAKED TIP BLADE

Because marine current turbines operate in water, cavitation is induced by blade tip vortex at high revolution speed. The tip vortex cavitation should be mitigated because it generally generates noise and vibration. To suppress tip vortex, turbine blades with rounded and raked tip were proposed. Two different shapes of raked tip turbines presented in Figure 7 were designed.

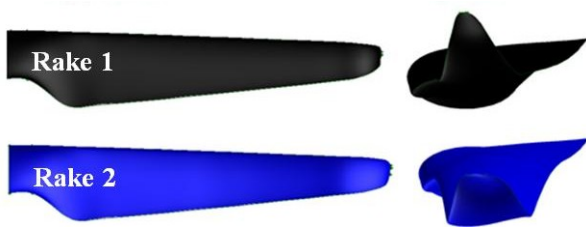


Figure 7; Shapes of raked turbine

In order to investigate the cavitation inception, the tip immersion was considered. Note that the cavitation number and pressure coefficient are defined as:

$$\sigma = (P_{AT} + \rho gh - P_v) / 0.5 \rho V^2 \quad (5)$$

$$C_{pressure} = (P_L - P_0) / 0.5 \rho V^2$$

where P_L is the local pressure. Cavitation occurs when the local negative pressure coefficient reaches the cavitation number. The tip immersion where the cavitation starts to take place is shown in Table 2. It is obvious that the raked tip's immersion depth is much less than the original, suggesting that the cavitation is delayed. Even with the cavitation delay, the power performance was not influenced, and actually showed a little increase at low TSR's as shown in Figure 8.

Table 2: Hub and tip immersion for cavitation inception

Turbine	Hub Immersion (m)	Tip Immersion (m)	Radius (m)
model	12.0	8.0	4.0
Rake 1	10.55	6.6	3.95
Rake 2	9.9	5.9	4.0

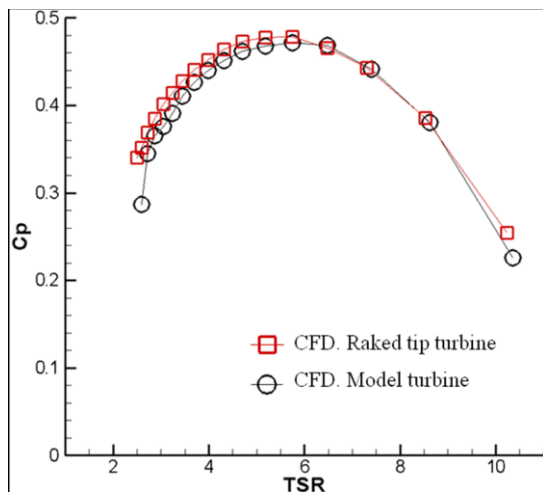


Figure 8: Comparison of power coefficient between reference turbine and tip raked turbine

7 CONCLUSIONS

The performance analysis methods for the design of marine current turbines were developed using both computational and experimental methods. BEMT and CFD methods for the computational analysis were validated against existing computational and experimental results. Open water tests for the model turbine were performed in a towing tank for the experimental analysis.

The results using both the computational and experimental methods were compared to each other and showed good correlation. Based on the validated CFD method, the performance analysis of newly proposed turbines with raked tip blades was performed. Its cavitation inception was much delayed compared to the original turbine without losing its power performance.

REFERENCES

- Bahaj, A. S., Molland, A. F., Chaplin, J. R. & Batten, W. M. J. (2007). 'Power and thrust measurements of marine current turbines under various hydrodynamic flow conditions in a cavitation tunnel and a towing tank'. *Renewable Energy* **32**, pp. 407-426.
- Baltazar, J. & Falcao de Campos, J. A. C. (2009). 'Unsteady analysis of a horizontal axis marine current turbine in yawed inflow conditions with a panel method'. *First International Symposium on Marine Propulsors smp'09*, Trondheim, Norway.
- Batten, W. M. J. & Bahaj, A. S. (2008). 'The prediction of the hydrodynamic performance of marine current turbines'. *Renewable Energy* **33**(5), pp. 1085-1096.
- Buhl, M. (2009). 'WT_Perf user's guide'. *Technical Report*. National Renewable Energy Laboratory, Colorado, United States.
- Carlton, J. S. (1994). *Marine propellers and propulsion*. Butterworth, Heinemann.
- Coiro, D. P., Maisto, U., Melone, S. & Grasso, F. (2006). 'Horizontal Axis Tidal Current Turbine: Numerical and Experimental Investigation'. *Proceeding of offshore wind and other marine renewable energies in Mediterranean and European seas*, European seminar, Rome, Italy.
- Harrison, M. E. (2009). 'A comparison between CFD simulations and experiments for predicting the far wake of horizontal axis tidal turbines'. *Proceeding of the 8th European Wave and Tidal Energy Conference*, Uppsala, Sweden.
- Khan, M. J., Bhuyan, G., Iqbal, M. T. & Quaicoe, J. E. (2009). 'Hydrokinetic energy conversion systems and assessment of horizontal and vertical axis turbines for river and tidal applications: A technology status review'. *Applied Energy* **86**(10), pp. 1823-1835.
- Kinnas, S. A. & Xu, W. (2009). 'Analysis of tidal turbines with various numerical methods'. *1st Annual MREC Technical Conference*, Massachusetts, USA.
- Liu, P. (2010). 'A computational hydrodynamics method for horizontal axis turbine – Panel method modeling migration from propulsion to turbine energy'. *Energy* **35**, pp. 2843-2851.
- Mason-Jones, A., Doherty, T. O', Doherty, D. M. O', Evans, P. S. & Wooldridge, C. F. (2008). 'Characterization of a HATT using CFD and ADCP site data'. *Proceedings of World Renewable Energy Congress*, Glasgow, UK.

- McCombes, T., Johnstone, C. & Grant, A. (2009). 'Unsteady 3D Wake Modeling for Marine Current Turbines'. Proceedings of the 8th European Wave and Tidal Energy Conference, Uppsala, Sweden.
- McLeod, A., Barnes, S., Rados, K. G. & Bryden, I. G. (2002). 'Wake effects in tidal current turbine farms'. Proceedings of international conference of marine renewable energy, Newcastle, UK.
- Viterna, L. A. & Corrigan, R. D. (1978). 'Fixed pitch rotor performance of large horizontal axis wind turbine'. DOE/NASA Workshop on Large Horizontal Axis Wind Turbines, Cleveland, Ohio.